

# A blob detector in color images \*

Anlong Ming

Beijing Key Laboratory of Intelligent  
Telecommunications Software and Multimedia,  
School of Computer Science and Technology,  
Beijing Univ. of Posts and Telecommunications  
Beijing 100876, China  
anthonyming@gmail.com

Huadong Ma

Beijing Key Laboratory of Intelligent  
Telecommunications Software and Multimedia,  
School of Computer Science and Technology,  
Beijing Univ. of Posts and Telecommunications  
Beijing 100876, China  
mhd@bupt.edu.cn

## ABSTRACT

In this paper, we propose a novel and efficient framework for the extension of multi-scale blob detection for the color domain to prevent information loss due to gray scale transformation and to allow us to exploit the photometric information. The framework also works well in gray scale space, it is mostly composed of i) a weighted multi-scale blob detector using a hybrid Laplacian and determinant of the Hessian operator, ii) a blob filter, includes a color-based Forstner operator for roundness calculation and a hue-based color histogram. The experimental results on stamp images in blob detection demonstrate the effectiveness of our proposed detector.

## Categories and Subject Descriptors

H.3.3 [Information Storage and Retrieval]: Information Search and Retrieval – Search Process; H.5.0 [Information Storage and Retrieval]: Information Interfaces and Presentation – General

## General Terms

Algorithms, Design, Performance

## Keywords

Blob, color, stamp image

## 1. INTRODUCTION

In the field of computer vision, a blob refers to a visual module with points (regions) in an image which is either

\*The work is supported by the National Natural Science Foundation of China (90612013), the National High Technology Research and Development Program of China under Grant No.2006AA01Z304, the Specialized Research Fund for the Doctoral Program of Higher Education (20050013010) and the NCET Program of MOE, China.

Permission to make digital or hard copies of all or part of this work for personal or classroom use is granted without fee provided that copies are not made or distributed for profit or commercial advantage and that copies bear this notice and the full citation on the first page. To copy otherwise, to republish, to post on servers or to redistribute to lists, requires prior specific permission and/or a fee.

CIVR'07, July 9–11, 2007, Amsterdam, The Netherlands.  
Copyright 2007 ACM 978-1-59593-733-9/07/0007 ...\$5.00.



**Figure 1:** (a) An example of five blobs in a red background, RGB value of the background is (255, 0, 0), RGB values of five blobs from left to right are (0, 130, 0), (158, 0, 255), (98, 80, 0), (0, 37, 255), (83, 36, 255). (b) The gray scale image converted from the left image with the same gray value 76.

brighter or darker than the surrounding [1, 2, 3]. Blob detection is usually the first step toward more complicated tasks, such as the determination of local deformations in images [1] or the extraction of scale-invariant interest points [2, 3]. Blob detection is often carried out through the computation of local extrema of some normalized derivatives of the linear scale-space image representation [1].

There are several motivations why blob detectors are studied and developed. One main reason is to provide complementary information about regions, which can not be obtained from edge detectors or corner detectors. In early works in this field, blob detection was used to obtain regions of interest for further processing. These regions could signal the presence of objects or parts with application to object recognition and/or object tracking. In other domains, such as histogram analysis, blob descriptors can also be used for peak detection with application to segmentation. Another common use of blob descriptors is the main primitives for texture analysis and recognition. In more recent works, blob descriptors have been found increasingly popular use as interest points for wide baseline stereo matching and to signal the presence of informative image features for appearance-based object recognition based on local image statistics. There is also the related notion of ridge detection to signal the presence of elongated objects.

However, most of blob detectors nowadays are studied in gray scale images while these detectors don't work well in color images with complex color background. Figure 1 gives an example of five blobs in a red background. The basic approach to computing color image derivatives is to calculate separately the derivatives of the channels and add them to produce the final color gradient. However, the derivatives of a color edge can be in the opposing directions for the separate color channels. Therefore, the summation of the derivatives per channel will discard the correlation between color channels.

In this paper, an adaptation of the tensor is used in blob detector. We propose a novel framework for the extension of multi-scale blob detection for the color domain to prevent information loss due to gray scale transformation and to allow us to exploit the photometric information. This detector also works well in gray scale space because we can easily extend gray scale space to 3 channels color space (e.g., in RGB color space, the gray value 76 can be denoted as  $(76, 76, 76)$ ). Further, because most blobs are quasi-circles, a color roundness calculation is given by an improved Forstner operator.

The remainder of the paper is organized as follows: Section 2 describes the related works, on which our results are based. Section 3 describes an interest blob detection scheme. Section 4 shows the experimental results and Section 5 concludes the paper.

## 2. RELATED WORKS

The work discussed in this paper mainly focuses on a multi-scale blob detector using an adaption of the color tensor.

### 2.1 Category of blob detection

Lots of blob detection approaches can roughly be grouped into the following categories [5]:

- Matched filters/template matching. These methods become less applicable when shape deformations appear or parameters of higher order transformations must be determined.
- Watershed detection [6]. These algorithms assume an image to be “gray value mountains” and simulate the process of rain falling onto the mountains, running down the mountain range and accumulating in valleys and basins. In practise, however, the bottleneck of these algorithms is the inherent noise sensitiveness which leads to the oversegmented results.
- Blob detection through scale-space analysis. We will discuss scale-space analysis in Section 2.1.
- Color tensor analysis followed by hypothesis testing of gradient directions [7, 8]. We will discuss the color tensor in Section 2.2.

### 2.2 Multi-scale blob detection

Scale space theory [1,9,10,11,12,13,14,15] is a framework for multi-scale signal representation developed by the computer vision, image processing and signal processing communities. It is a formal theory for handling image structures at different scales in such a way that fine-scale features can be successively suppressed and a scale parameter  $t$  can be associated with each level in the scale-space representation. In general, when a local image structure is present in a certain range of scales, the points are then detected at each scale within this range. As a consequence, there are many points, which represent the same structure, but the localization and the scale of the points is different. However, the unnecessarily high number of points increases the probability of mismatches and the complexity of matching and recognition algorithm. Therefore, methods for rejecting the false matches and for verifying the results are necessary at further steps of the algorithms.

- Laplacian of the Gaussian [1]. One of the first and also most common blob detectors is based on the Laplacian of the Gaussian.
- The difference of Gaussians (DoG) approach [16]. This operator is in essence similar to the Laplacian and can be viewed as an approximation of the Laplacian operator.
- The determinant of the Hessian (DoH) [1]. In simplified form, the determinant of the Hessian computed from Haar wavelets was used as a basic interest point operator in the SURF descriptor [2] for image matching and object recognition. Also, Christophe Damerval et al proposed an approach to blob detection based on wavelet transform modulus maxima [17].
- The hybrid Laplacian and determinant of the Hessian operator (Hessian-Laplace) [3]. A hybrid operator between the Laplacian and the determinant of the Hessian blob detectors was also proposed, where spatial selection is done by the determinant of the Hessian and scale selection is performed with the scale-normalized Laplacian.
- Affine-adapted differential blob detectors [15, 3, 18]. The blob descriptors obtained from these blob detectors with automatic scale selection are invariant to translations, rotations and uniform rescalings in the spatial domain.
- Gray-level blobs, gray-level blob trees and scale-space blobs [1]. A region with spatial extent defined from a watershed analogy was associated with each local maximum, as well a local contrast defined from a so-called delimiting saddle point. A local extremum with extent defined in this way was referred to as a gray-level blob. Moreover, by proceeding with the watershed analogy beyond the delimiting saddle point, a gray-level blob tree was defined to capture the nested topological structure of level sets in the intensity landscape, in the way that is invariant to affine deformations in the image domain and monotone intensity transformations. By studying how these structures evolve with increasing scales, the notion of scale-space blobs was introduced. Beyond local contrast and extent, these scale-space blobs also measured how stable image structures are in scale-space, by measuring their scale-space lifetime.
- Maximally stable extremum regions (MSER). Matas et al [19, 20, 21] were interested in defining image descriptors that are robust under perspective transformations. They studied level sets in the intensity landscape and measured how stable these were along the intensity dimension. Based on this idea, they defined a notion of maximally stable extremum regions and showed how these image descriptors can be used as image features for stereo matching.

The main drawback of these blob detectors is based on gray scale space. There are two major advantages of using color vision. First, color is an important discriminative property of objects, allowing us to distinguish between mustard and mayonnaise. Second, color provides extra information which allows the distinction among various physical causes

for color variations in the world, such as changes due to shadows, light source reflections, and object reflectance variations. This helps to quickly identify a black object on the road as a shadow.

### 2.3 Color tensor analysis

As a solution to color space mergence problem, DiZenzo [4] have proposed a color tensor, derived from the structure tensor, for computing the color gradient and extracting circular structures. This method extracts blobs by detecting distinct points and analyzing their circularity. In the first step, potential interest points are detected by analyzing and thresholding the eigenvalues of the structure tensor in the similar way as the classical Harris-Operator. The second step consists of calculating the gradient directions in the local neighborhood of a candidate point and estimating the common intersection point of all gradients assuming circularity. Finally, a hypothesis test on the intersections accuracy, i.e. the deviation of the gradient directions from the intersection point, decides about acceptance or rejection of the candidate point. This method has three distinctive advantages: ① It can be implemented efficiently using recursive filters with noise suppression embedded. ② It delivers subpixel precise results for blob center points. ③ It needs only a few parameters to be initialized.

However, the disadvantage of this method is its limitation in extracting circular structures only. The algorithm fails as soon as the gradients do not intersect in a common point, e.g. in the case of ellipses.

### 2.4 Our Work

Our work described in the following Section is mainly inspired by the pioneer work of Lindeberg [1], and the Forstner method [7] while our work extends it to more generic structures. In particular, our scheme is based on a scale space representation using a color-based hybrid of Laplacian and determinant of the Hessian operator where spatial selection is done by the determinant of the Hessian and scale selection is performed with the scale-normalized Laplacian. Furthermore, hue-based blob color histogram is proposed for filtering.

## 3. OUR BLOB DETECTOR

Our blob detection approach consists of four major steps. First, we select a Gaussian kernel for convolution. The second step is the extraction of blob points (Sect. 3.2). The third step outlined in Sect. 3.3 is selecting automatic scale around a given point. Finally, both extended Forstner operator for roundness detection and blob color histogram are given to filter quasi-blobs (Sect. 3.4).

### 3.1 A Gaussian Kernel for Multi-scale Representation

Given an input image  $f(x, y)$ , this image is convolved by a Gaussian kernel  $G(u, v, \sigma_I, \sigma_D)$  (we adopt this kernel instead of traditional one for its further symmetry):

$$G(u, v, \sigma_I, \sigma_D) = \frac{1}{2\pi\sigma_I} e^{-((u - (\frac{\sigma_D}{2}))^2 + (v - (\frac{\sigma_D}{2}))^2)/2\sigma_I} \quad (1)$$

where  $\sigma_I$  is the integration scale,  $\sigma_D$  is the differentiation

scale.

$$\begin{aligned} \sigma_I &= \xi^n \sigma_0 \\ \sigma_D &= s \sigma_I \\ 0 &\leq u < \sigma_D \\ 0 &\leq v < \sigma_D \end{aligned}$$

$\xi$  is the scale factor between successive levels (set to 1.4 [15, 16]),  $s$  is a constant factor (set to 0.7 in our experiments). Then we can get a scale-normalized Gaussian kernel  $\nabla_{norm} G(\sigma_I)$  after the equation (1) is normalized.

### 3.2 Extraction of Blob Points.

To get better detection result, we improve color contrast for the given image  $f(x, y)$  in HSI color space. It means that hues remain unchanged while saturation and intensity increase. Let  $F(x, y) = (F_R(x, y), F_G(x, y), F_B(x, y))$  represents the image after it has been improved color contrast and converted to RGB color space. Then Hessian Matrix  $H$  (not to be confused with the structure tensor) is denoted as

$$H(x, y) = \begin{vmatrix} F_{xx} & F_{xy} \\ F_{yx} & F_{yy} \end{vmatrix}$$

with the second partial derivatives  $F_{xx}, F_{yy}, F_{xy} = F_{yx}$ , where

$$\begin{aligned} F_{xx} &= \omega_1 F_{R_{xx}} + \omega_2 F_{G_{xx}} + \omega_3 F_{B_{xx}} \\ F_{yy} &= \omega_1 F_{R_{yy}} + \omega_2 F_{G_{yy}} + \omega_3 F_{B_{yy}} \\ F_{xy} &= F_{yx} = \omega_1 F_{R_{xy}} + \omega_2 F_{G_{xy}} + \omega_3 F_{B_{xy}} \end{aligned}$$

The basic approach to computing color image derivatives is to calculate separately the derivatives of the channels and add them to produce the final color gradient. However, the derivatives of a color edge can be in the opposing directions for the separate color channels. So we weight color by the contributions of different channels, and  $\omega_1, \omega_2, \omega_3$  are the weighted parameters,  $\omega_1 + \omega_2 + \omega_3 = 1$ . In our experiment,  $\omega_1 = \frac{r}{r+g+b}$ ,  $\omega_2 = \frac{g}{r+g+b}$ , and  $\omega_3 = \frac{b}{r+g+b}$ .

In  $H(x, y)$  above,

$$\begin{aligned} F_{R_{xx}} &= F_R(x+1, y) + F_R(x-1, y) - 2 * F_R(x, y) \\ F_{G_{xx}} &= F_G(x+1, y) + F_G(x-1, y) - 2 * F_G(x, y) \\ F_{B_{xx}} &= F_B(x+1, y) + F_B(x-1, y) - 2 * F_B(x, y) \\ F_{R_{yy}} &= F_R(x, y+1) + F_R(x, y-1) - 2 * F_R(x, y) \\ F_{G_{yy}} &= F_G(x, y+1) + F_G(x, y-1) - 2 * F_G(x, y) \\ F_{B_{yy}} &= F_B(x, y+1) + F_B(x, y-1) - 2 * F_B(x, y) \\ F_{R_{xy}} &= F_R(x+1, y+1) + F_R(x, y) - F_R(x, y+1) - F_R(x+1, y) \\ F_{G_{xy}} &= F_G(x+1, y+1) + F_G(x, y) - F_G(x, y+1) - F_G(x+1, y) \\ F_{B_{xy}} &= F_B(x+1, y+1) + F_B(x, y) - F_B(x, y+1) - F_B(x+1, y) \end{aligned}$$

By considering the scale-normalized Laplacian operator

$$\nabla_{norm} detHL(x, y, \sigma_I) = \nabla_{norm} G(\sigma_I) * \begin{bmatrix} F_{xx} & F_{xy} \\ F_{yx} & F_{yy} \end{bmatrix} \quad (2)$$

where HL denotes the Hessian of Laplace to detect scale-space maxima/minima of this operator.

$$(\tilde{x}, \tilde{y}) = \arg \max_{min} local_{(x,y)} (\nabla_{norm} detHL(x, y, \sigma_0)) \quad (3)$$

The blob points  $(\tilde{x}, \tilde{y})$  are defined from an operational differential geometric definitions that leads to blob descriptors that are covariant with translations, rotations and rescalings in the image domain. In simplified form, the determinant of the Hessian computed from Haar wavelets is used as a basic interest point operator in the SURF descriptor [2] for image matching and object recognition.

### 3.3 Automatic Scale Selection

At a certain scale  $\sigma_I$  for a given scale-space representation in an image  $F(x, y)$  with 3 channels mentioned above,

$$\nabla_{norm} L(x, y, \sigma_I) = \nabla_{norm} G(\sigma_I) * F(x, y) \quad (4)$$

Then, A straightforward way to obtain a multi-scale blob detector with automatic scale selection is to consider the scale-normalized Laplacian operator

$$\nabla_{norm}^2 L(x, y, \sigma_I) = \sigma_I (L_{xx} + L_{yy}) = \sigma_I L_{xx} + \sigma_I L_{yy} \quad (5)$$

where

$$\begin{aligned} \sigma_I L_{xx} &= \nabla_{norm} G(\sigma_I) * F_{xx} \\ \sigma_I L_{yy} &= \nabla_{norm} G(\sigma_I) * F_{yy} \\ F_{xx} &= \omega_1 F_{R_{xx}} + \omega_2 F_{G_{xx}} + \omega_3 F_{B_{xx}} \\ F_{yy} &= \omega_1 F_{R_{yy}} + \omega_2 F_{G_{yy}} + \omega_3 F_{B_{yy}} \end{aligned} \quad (6)$$

So

$$\nabla_{norm}^2 L(x, y, \sigma_I) = \nabla_{norm} G(\sigma_I) * F_{xx} + \nabla_{norm} G(\sigma_I) * F_{yy} \quad (7)$$

Then scale selection is performed with the scale-normalized Laplacian

$$\widetilde{\sigma}_D = s\widetilde{\sigma}_I = s(\arg\max_{\min local \sigma_I} (\nabla_{norm}^2 L(\widetilde{x}, \widetilde{y}, \sigma_I))) \quad (8)$$

This operator has been used for image image matching, object recognition as well as texture analysis.

### 3.4 Interesting Blob Filter

#### 3.4.1 Extended Forstner Operator for Roundness Detection

Given a point  $(\widetilde{x}, \widetilde{y})$ , the image  $F(x, y)$  and the scale  $\widetilde{\sigma}_D$ , we consider the matrix in RGB color space

$$Q = N^{-1} = \begin{bmatrix} \sum F_u^2 & \sum F_u F_v \\ \sum F_v F_u & \sum F_v^2 \end{bmatrix}^{-1} \quad (9)$$

where

$$\begin{aligned} \sum F_u^2 &= \omega_1 \sum_{i=\widetilde{x}-\widetilde{\sigma}_D}^{\widetilde{x}+\widetilde{\sigma}_D-1} \sum_{j=\widetilde{y}-\widetilde{\sigma}_D}^{\widetilde{y}+\widetilde{\sigma}_D-1} (F_R(x+1, y+1) - F_R(x, y))^2 \\ &+ \omega_2 \sum_{i=\widetilde{x}-\widetilde{\sigma}_D}^{\widetilde{x}+\widetilde{\sigma}_D-1} \sum_{j=\widetilde{y}-\widetilde{\sigma}_D}^{\widetilde{y}+\widetilde{\sigma}_D-1} (F_G(x+1, y+1) - F_G(x, y))^2 \\ &+ \omega_3 \sum_{i=\widetilde{x}-\widetilde{\sigma}_D}^{\widetilde{x}+\widetilde{\sigma}_D-1} \sum_{j=\widetilde{y}-\widetilde{\sigma}_D}^{\widetilde{y}+\widetilde{\sigma}_D-1} (F_B(x+1, y+1) - F_B(x, y))^2 \\ \sum F_v^2 &= \omega_1 \sum_{i=\widetilde{x}-\widetilde{\sigma}_D}^{\widetilde{x}+\widetilde{\sigma}_D-1} \sum_{j=\widetilde{y}-\widetilde{\sigma}_D}^{\widetilde{y}+\widetilde{\sigma}_D-1} (F_R(x, y+1) - F_R(x+1, y))^2 \\ &+ \omega_2 \sum_{i=\widetilde{x}-\widetilde{\sigma}_D}^{\widetilde{x}+\widetilde{\sigma}_D-1} \sum_{j=\widetilde{y}-\widetilde{\sigma}_D}^{\widetilde{y}+\widetilde{\sigma}_D-1} (F_G(x, y+1) - F_G(x+1, y))^2 \\ &+ \omega_3 \sum_{i=\widetilde{x}-\widetilde{\sigma}_D}^{\widetilde{x}+\widetilde{\sigma}_D-1} \sum_{j=\widetilde{y}-\widetilde{\sigma}_D}^{\widetilde{y}+\widetilde{\sigma}_D-1} (F_B(x, y+1) - F_B(x+1, y))^2 \\ \sum F_u F_v &= \sum F_v F_u = \\ &\omega_1 \sum_{i=\widetilde{x}-\widetilde{\sigma}_D}^{\widetilde{x}+\widetilde{\sigma}_D-1} \sum_{j=\widetilde{y}-\widetilde{\sigma}_D}^{\widetilde{y}+\widetilde{\sigma}_D-1} (F_R(x, y+1) - F_R(x+1, y)) \\ &(F_R(x, y+1) - F_R(x+1, y)) \\ &+ \omega_2 \sum_{i=\widetilde{x}-\widetilde{\sigma}_D}^{\widetilde{x}+\widetilde{\sigma}_D-1} \sum_{j=\widetilde{y}-\widetilde{\sigma}_D}^{\widetilde{y}+\widetilde{\sigma}_D-1} (F_G(x, y+1) - F_G(x+1, y)) \\ &(F_G(x, y+1) - F_G(x+1, y)) \\ &+ \omega_3 \sum_{i=\widetilde{x}-\widetilde{\sigma}_D}^{\widetilde{x}+\widetilde{\sigma}_D-1} \sum_{j=\widetilde{y}-\widetilde{\sigma}_D}^{\widetilde{y}+\widetilde{\sigma}_D-1} (F_B(x, y+1) - F_B(x+1, y)) \\ &(F_B(x, y+1) - F_B(x+1, y)) \end{aligned}$$

Then roundness  $q$  of a color blob is denoted as

$$q = \frac{4 * detN}{(traceN)^2} \quad (10)$$

#### 3.4.2 Blob Color Histogram

The blob color histogram of an image is built by counting the number of blobs of each average color. The most common RGB space is not used in this work because it is not perceptually uniform [22, 23, 24]. HSI is adopted here to characterize different colors because the transformation from RGB space is nonlinear but easily invertible.

However, HSI brings about the disadvantage that hue is singular at the chromatic axis  $R \approx G \approx B$  or  $S \approx 0$ . Three gray colors are introduced to solve this problem. The color quantization algorithm in this work is similar to that of [22].

Therefor, we use 12 hues, including three channel colors, the number of the colors is 36. Let  $B$  be the set of detected blobs and a blob  $b \in B$ , and  $C(b) = i$  ( $i = 0, 1, \dots, 35$ ) if and only if the hue of  $b$  is  $i$ . Then we can define 36 sets of  $I(i) = \{C(a) = i, \forall a \in B\}$ .

We define  $H(i)$  as the number of elements of set  $I(i)$ . Then we define reference hue of blobs in set  $B$ , as  $\zeta(B)$

$$\zeta(B) = i = \arg \max_i (H(i)) \quad (11)$$

#### 3.4.3 Filter

Then we can build a filter according to the definition in Section 1. Let  $b \in B$ , the roundness of  $b$  is  $q$ , then interesting blobs filter  $\Gamma(b)$  is

$$\Gamma(b) = \begin{cases} 1, & q > T_q \text{ and } C(b) = \zeta(B) \\ 0, & \text{otherwise} \end{cases} \quad (12)$$

where  $T_q$  is a constant factor ( $T_q = 0.6$  in our experiments).

### 3.5 The Integrated Algorithm

The integrated algorithm of our detector is described as Algorithm 1.

---

**Algorithm 1** The multi-scale blob detector in color space

---

**Input:**  $F(x, y)$ ,  $q_0$ ,  $\sigma_0$ ,  $s$   $\{F(x, y)$  is a color image.  $q_0$  is the threshold of roundness. $\}$

**Output:**  $R$   $\{R$  is the set of detected blobs. $\}$

- 1: Initialize setting, a blob set  $R = NULL$
  - 2: Extract blob points (see Section 3.2).
  - 3: Compute automatic scales (see Section 3.3), get the result of detected blobs: set  $B$ .
  - 4: Compute  $\zeta(B)$ .
  - 5: **for all**  $b \in B$  **do**
  - 6:   **if**  $q > q_0$  and  $C(b) = \zeta(B)$  **then**
  - 7:      $b$  is an interesting blob, append  $b$  to  $R$ .
  - 8:   **end if**
  - 9:   Return  $R$
  - 10: **end for**
- 

## 4. EXPERIMENTAL RESULTS

### 4.1 Experimental Environment

We test our method on a set of 5 Chinese stamp images. These images are scanned from a common scanner. Intel <sup>®</sup> Open Source Computer Vision Library (OpenCv) is used in our experiment for image preprocessing. The interest blobs in these images are defined as:

- The interest blobs are quasi-circles.
- The color of the interest blobs is approximative.

## 4.2 Performance Evaluation

The right interest blobs detected in 5 Chinese stamp images by two different methods is shown in figure 2. According to the results shown in figure 3 (a), (b), (c), we can initialize the input parameters as:  $q_0 = 0.7$ ,  $\sigma_0 = 1.4$ ,  $s = 0.7$ .

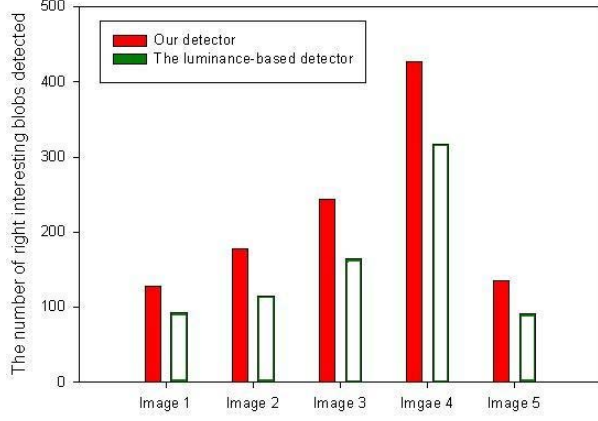


**Figure 2:** The right interest blobs detected respectively by our detector and the luminance-based blob detector (the Laplacian of the Gaussian) in 5 Chinese stamp images.

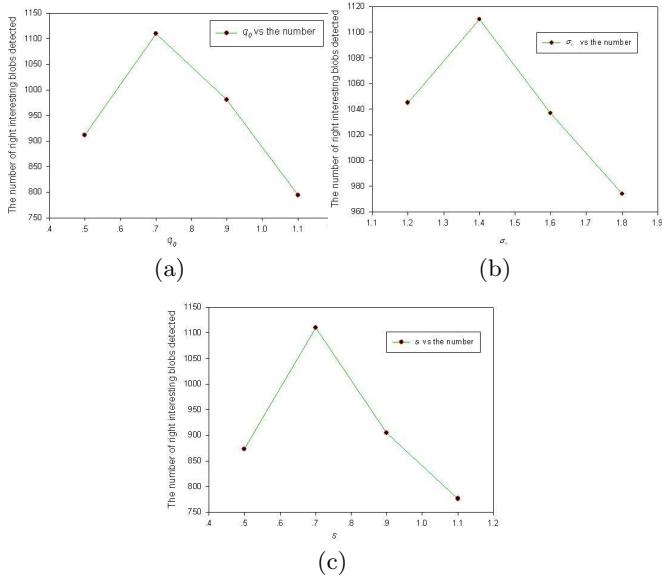


**Figure 3:** (a) The case with  $\sigma_0 = 1.4$ ,  $s = 0.7$ . (b) The case with  $q_0 = 0.7$ ,  $s = 0.7$ . (c) Where  $q_0 = 0.7$ ,  $\sigma_0 = 1.4$ .

## 4.3 Analysis

In figure 4, five stamp images for the interesting blob detection are given. Our method achieve much better results



(a)



(b)



(c)



(d)



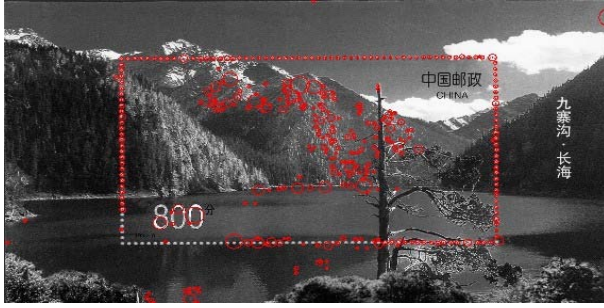
(e)

**Figure 4:** (a) ~ (e) 5 stamp images.

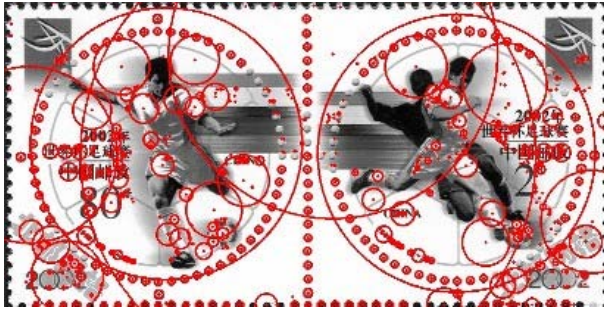




(a)



(b)



(c)



(d)



(e)



(a)



(b)



(c)



(d)



(e)

Figure 5: (a) ~ (e) Detected blobs based on luminance in gray scale space using the Laplacian of the Gaussian.

Figure 6: (a) ~ (e) Detected interesting blobs based on our method in color space.

(see figure 6) than that of luminance-based blob detection method (see figure 5).

- The corruption of the traditional luminance-based blob detection method is originated from information loss due to gray scale transformation. Color is an important discriminative property of objects, allowing us to distinguish between background and objects, and color provides extra information which allows the distinction while the traditional luminance-based blob detection method fails to work on color.
- We give a blob detector in the complex background using the roundness computing by the extended forstner operator. The detected blobs are quasi-circles with approximated color.
- Coincidentally, The blob color histogram ensures that the most of these detected blobs are on the segmentation curves of the stamp images.

## 5. CONCLUSION AND FUTURE WORK

In this paper, we propose a novel framework to detect interesting blobs in the color domain. To solve information loss due to gray scale transformation, we extend the traditional luminance-based blob detection method to the color-based method. In particular, we give a color-based Forstner operator for the calculation of blob roundness and a hue-based blob color histogram definition, which work well in interesting blob filtering.

However, some factors such as shadow-shading distortion are not considered in this paper. Detection of other features in color space is our future work.

## 6. REFERENCES

- [1] Lindeberg, Tony: Feature detection with automatic scale selection, *International Journal of Computer Vision*, Vol. 30, Issue 2 (1998) 77-116.
- [2] H. Bay, T. Tuytelaars and L. van Gool. SURF.: Speeded Up Robust Features. In *Proceedings of the 9th European Conference on Computer Vision*, Springer LNCS, Vol 3951, Issue 1 (2006) 404-417.
- [3] Mikolajczyk, K. and Schmid, C.: Scale and affine invariant interest point detectors. *International Journal of Computer Vision*, Vol 60 Issue 1 (2004) 63-86.
- [4] Weijer, V., Gevers, T. and Arnold W. M Smeulders.: Robust Photometric Invariant Features From the Color Tensor Joost. *IEEE Transactions on Image Processing*, Vol.15, No.1 (2006)
- [5] Hinz, S: Fast and subpixel precise blob detection and attribution, *IEEE International Conference on Image Processing*, Vol.3, Issue 3 (2005) 457-60.
- [6] C. Steger: Subpixel-Precise Extraction of Watersheds, *7th International Conference on Computer Vision* (1999) 884-890.
- [7] W. Forstner and E. Gulch: A Fast Operator for Detection and Precise Location of Distinct Points, Corners, and Circular Features, *Proceedings of ISPRS Intercommission Workshop*, Interlaken, Switzerland (1987)
- [8] U. Koethe, Edge and Junction: Detection with an Improved Structure Tensor, in *Pattern Recognition*, *Lecture Notes in Computer Science*, Springer-Verlag (2003) 25-32.
- [9] Witkin, A. P.: Scale-space filtering, *Proceedings of 8th International Joint Conference on Art. Intell.*, Karlsruhe, Germany (1983) 1019C1022.
- [10] Koenderink, Jan: The structure of images, *Biological Cybernetics*, Vol. 50 (1984) 363-370.
- [11] Lindeberg, Tony: *Scale-Space Theory in Computer Vision*, Kluwer Academic Publishers, ISBN 0-7923-9418-6 (1994)
- [12] Florack, Luc: *Image Structure*, Kluwer Academic Publishers (1997)
- [13] Sporring, Jon et al: *Gaussian Scale-Space Theory*, Kluwer Academic Publishers (1997)
- [14] Romeny, Bart ter Haar: *Front-End Vision and Multi-Scale Image Analysis*, Kluwer Academic Publishers (2003)
- [15] Lindeberg, Tony: Edge detection and ridge detection with automatic scale selection, *International Journal of Computer Vision*, Vol. 30, Issue 2 (1998) 117-154.
- [16] Lowe, D. G.: Distinctive Image Features from Scale-Invariant Keypoints. *International Journal of Computer Vision*, Vol. 60, Issue. 2 (2004) 91-110.
- [17] Christophe Damerval and Sylvain Meignen.: Blob Detection With Wavelet Maxima Lines. *IEEE Signal Processing Letters* (2006)
- [18] Baumberg, A.: Reliable feature matching across widely separated views. *Proceedings of IEEE Conference on Computer Vision and Pattern Recognition* (2000) 1774-1781.
- [19] Matas, J., Burianek, J., and Kittler, J.: Object Recognition using the Invariant Pixel-Set Signature. In *Proceedings of the British Machine Vision Conference*, London, UK (2000) 606-615.
- [20] Matas, J., Chum, O., Urban, M., and Pajdla, T.: Robust wide baseline stereo from maximally stable extremum regions. *British Machine Vision Conference* (2002) 384-393.
- [21] Matas, J., Chum, O., Urban, M., and Pajdla, T.: Robust wide-baseline stereo from maximally stable extremal regions. *Image and Vision Computing* Vol. 22, Issue 10 (2004) 761-767.
- [22] Smith, J.R. and Chang, S.: Single color extraction and image query. In: *Proc. of IEEE Intl Conf. on Image Processing* (1995) 528-531.
- [23] C. Carson, S. Belongie, H. Greenspan, and J. Malik: Blobworld: Image Segmentation Using Expectation-Maximization and Its Application to Image Querying, *IEEE Trans. on Pattern Analysis and Machine Intelligence*, vol. 24, Issue 8 (2002) 1026-1038
- [24] A. Mojsilovic, J. Hu, and E. Soljanin: Extraction of perceptually important colors and similarity measurement for image matching retrieval and analysis, *IEEE Trans. on Image Processing*, Vol. 11, Issue 11 (2002) 1238-1248